Ecological Monographs, 86(1), 2016, pp. 125–144

Quantifying demographic uncertainty: Bayesian methods for integral projection models

Bret D. Elderd[1,3] and Tom E. X. Miller[2]

[1]*Department of Biological Sciences, Louisiana State University, Baton Rouge, Louisiana 70803 USA*
[2]*Department of BioSciences, Program in Ecology and Evolutionary Biology, Rice University, Houston, Texas 77005 USA*

Abstract. Integral projection models (IPMs) are a powerful and popular approach to modeling population dynamics. Generalized linear models form the statistical backbone of an IPM. These models are typically fit using a frequentist approach. We suggest that hierarchical Bayesian statistical approaches offer important advantages over frequentist methods for building and interpreting IPMs, especially given the hierarchical nature of most demographic studies. Using a stochastic IPM for a desert cactus based on a 10-year study as a worked example, we highlight the application of a Bayesian approach for translating uncertainty in the vital rates (e.g., growth, survival, fertility) to uncertainty in population-level quantities derived from them (e.g., population growth rate). The best fit demographic model, which would have been difficult to fit under a frequentist framework, allowed for spatial and temporal variation in vital rates and correlated responses to temporal variation across vital rates. The corresponding posterior probability distribution for the stochastic population growth rate (λ_S) indicated that, if current vital rates continue, the study population will decline with nearly 100% probability. Interestingly, less supported candidate models that did not include spatial variance and vital rate correlations gave similar estimates of λ_S. This occurred because the best fitting model did a much better job of fitting vital rates to which the population growth rate was weakly sensitive. The cactus case study highlights several advantages of Bayesian approaches to IPM modeling, including that they: (1) provide a natural fit to demographic data, which are often collected in a hierarchical fashion (e.g., with random variance corresponding to temporal and spatial heterogeneity); (2) seamlessly combine multiple data sets or experiments; (3) readily incorporate covariance between vital rates; and, (4) easily integrate prior information, which may be particularly important for species of conservation concern where data availability may be limited. However, constructing a Bayesian IPM will often require the custom development of a statistical model tailored to the peculiarities of the sampling design and species considered; there may be circumstances under which simpler methods are adequate. Overall, Bayesian approaches provide a statistically sound way to get more information out of hard-won data, the goal of most demographic research endeavors.

Key words: demography; hierarchical Bayes; IPMs; Markov Chain Monte Carlo; model selection; parameter estimation; population dynamics; process error; stochasticity; uncertainty.

Introduction

Dynamic population models are a valuable tool for researchers to ask and answer questions of ecological, evolutionary, and conservation concern. Their utility becomes especially apparent when asking questions of an applied nature. For instance, population models have been used extensively to examine the growth and spread of invasive and endangered species (e.g., McEvoy and Coombs 1999, Franklin et al. 2000, Parker 2000) and to design species management plans (e.g., Crouse et al. 1987, Doak 1995). Within the realm of population models, there is a wide variety to choose from. The type of model chosen is partially determined by the questions asked and the data available. The spectrum of analyses range from count-based approaches that directly track population change (Dennis et al. 1991) to individual-based models that predict population dynamics derived from the fates of individuals (Grimm 2005). Between these two extremes lay matrix models, which have been broadly adopted since first introduced (Leslie 1945, Lefkovitch 1965).

Matrix models, like all methods, have their limitations. A well-recognized problem with constructing a matrix model is how to best divide individuals into age, size, or stage classes (Vandermeer 1978, Moloney 1986). Integral projection models (IPMs) present a solution to this problem by assuming that individuals within a population exist along a continuous spectrum of one or more quantitative traits, most often size (Easter-

Manuscript received 17 August 2015; accepted 14 September 2015; final version received 12 October 2015. Corresponding Editor: N. T. Hobbs.

[3]E-mail: elderd@lsu.edu

ling et al. 2000, Rees and Ellner 2009, Coulson 2012, Metcalf et al. 2013, Merow et al. 2014*a*, Rees et al. 2014). This avoids the often arbitrary division of discrete classes associated with matrix models while reducing the number of parameters that need to be estimated from the data (Easterling et al. 2000, Ellner and Rees 2006). Given the advantages of IPMs, they have been rapidly adopted (e.g., Williams and Crone 2006, Coulson et al. 2011, Miller et al. 2012, Wallace et al. 2013), expanded upon (Kuss et al. 2008, Williams et al. 2012), and summarized by recent how-to guides (Ellner and Rees 2006, Coulson 2012, Metcalf et al. 2013, Merow et al. 2014*a*, Rees et al. 2014).

Generalized linear models (GLMs), either fixed-effects GLMs or "mixed" models that include fixed and random effects (GLMMs: Bolker et al. 2009), form the backbone of most IPMs, providing a framework to predict demographic vital rates (e.g., survival, growth, reproductive output) based on continuous state variables such as size. Note that the IPMs discussed here differ from "integrated projection models", another demographic technique with the same acronym (Kéry and Schaub 2012). Integrated projection models combine demographic data with population count data (Davis et al. 2014). For IPMs, the vital rate GLMs or GLMMs have most often been fit using frequentist or maximum likelihood statistical approaches. Recently, a few IPM studies have employed Bayesian statistical methods to estimate vital rate functions (Rees and Ellner 2009, Diez et al. 2014, Merow et al. 2014*b*, Ohm and Miller 2014). A general overview of why and how one would use a Bayesian approach to integral projection modeling is currently lacking. A goal of this paper is therefore to provide such an overview, including a worked example and corresponding code (see Appendix) of an IPM parameterized using a Bayesian approach.

Before delving deeper into the motivation for a Bayesian approach, we first need to define it. Bayes' theorem states that:

$$P(\theta \mid \text{Data}) \propto \pi(\theta)\, L(\text{Data} \mid \theta) \tag{1}$$

where the posterior probability of the model parameters θ given the data is proportional to the prior probability of the parameters $\pi(\theta)$ times the likelihood of the data given the parameters $L(\text{Data} \mid \theta)$. Because the posterior probability is typically "sampled" numerically rather than calculated analytically, its estimation can be computationally complex. However, the development and availability of freeware programs (e.g., WinBugs, OpenBugs, JAGS, and STAN) and a proliferation of ecologically oriented books (e.g., Clark 2007, McCarthy 2007, Kéry 2010, King et al. 2010, Link and Barker 2010, Hobbs and Hooten 2015) have made Bayesian analysis broadly accessible to ecologists. In the context of integral projection modeling, the goal of a Bayesian approach would be to generate posterior distributions for the vital rate parameters θ, which provide the "instructions" for population dynamics. Using estimates of the vital rate parameters, posterior distributions of other metrics associated with the IPMs such as population growth rate and its sensitivities can be easily derived, as we demonstrate below.

Relative to the more common frequentist and maximum likelihood approaches, hierarchical Bayesian approaches provide greater flexibility in fitting vital rate models, allowing for more realistic error structures (for all parameters, not just "response" variables) and the ability to accommodate multiple data sets. The basic process consists of specification of the vital rate models, Bayesian analysis of the vital rate models, and building the IPM given the vital rate results (Fig. 1). We suggest and emphasize throughout that a Bayesian approach provides several important advantages in the construction and analysis of IPMs that strengthen the biological inferences gleaned from the data, although all these advantages may come at the cost of greater time and effort required to custom-build these models.

Bayesian methods provide a natural fit for demographic modeling in general (Hobbs et al. 2015) and for IPMs in particular for several reasons. First, intentionally or not, demographic data are typically collected in a hierarchical fashion, including multiple individuals tracked longitudinally across multiple years, spanning plot- and site-level spatial variation. Thus, in addition to "observation error", there is biologically meaningful random variance, or "process error", associated with individual identity, time, and space. These sources of variation can be accounted for even if the underlying mechanisms have not been identified (e.g., which climatic factors cause year-to-year fluctuations). Although maximum likelihood-based approaches can be used to account for some types of random variance in vital rates (e.g., Williams and Crone 2006, Rees and Ellner 2009), they tend to break down for hierarchically rich models with multiple, nested sources of variance; Bayesian methods, by contrast, are ideally suited for hierarchical data (i.e., "hierarchical Bayes", Gelman and Hill 2007).

A second advantage of Bayesian analysis is the ease of combining multiple data sets or experiments (Clark 2003, Clark et al. 2005, Clark and Gelfand 2006, Hanks et al. 2011, Elderd et al. 2013, Davis et al. 2014). A vast majority of ecological processes are best described by linking multiple sets of data, which is easily done under a Bayesian framework (Hille Ris Lambers et al. 2005, Ladeau and Clark 2006, Cressie et al. 2009). Demographic models must capture the entire, potentially complex life cycle of the study organism; this will often require that demographers cobble together independent observations from different components of the life cycle. We suggest that the ability to analyze multiple, independent data sets within a single framework is a key advantage for the construction and anal-

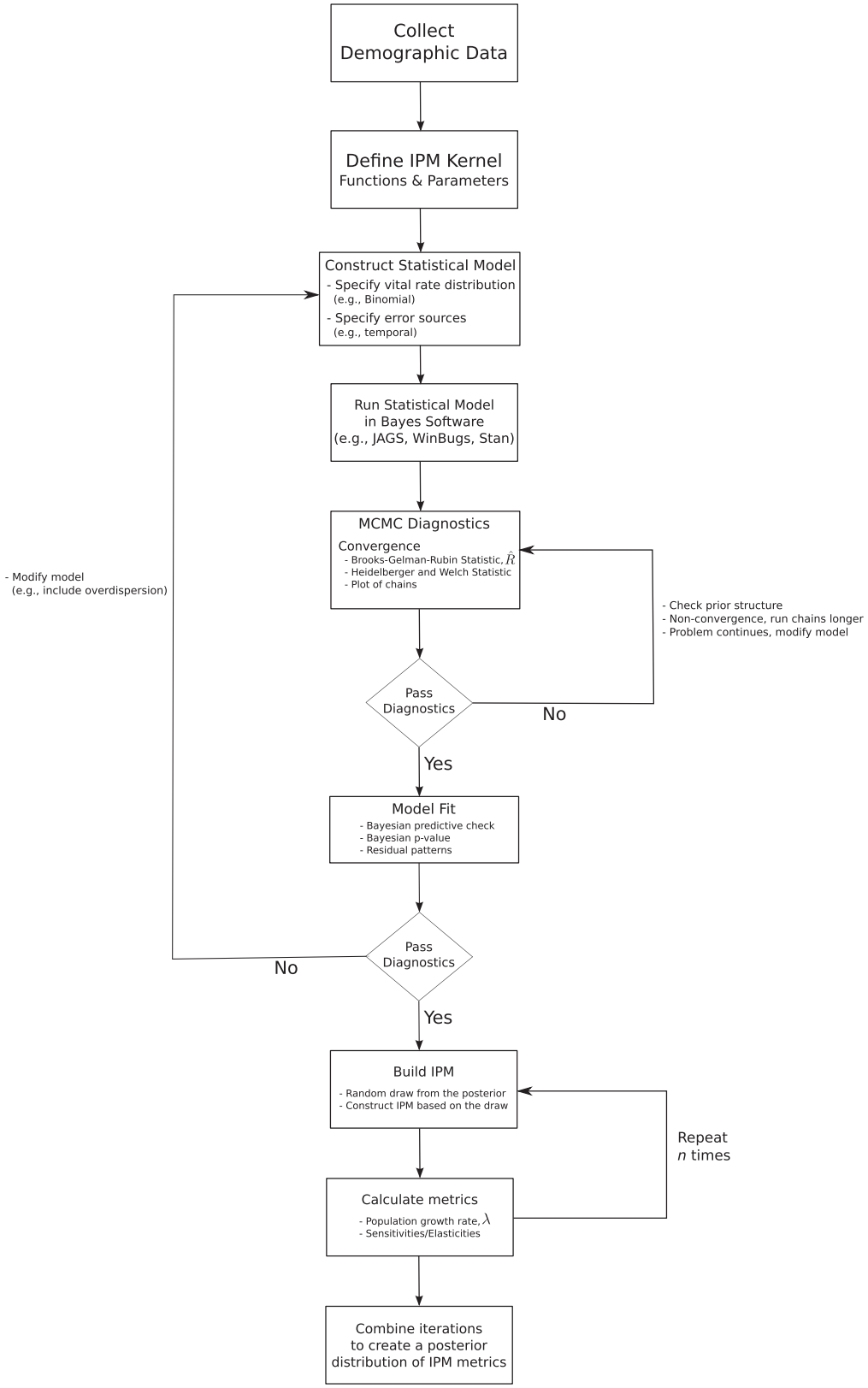

FIG. 1. Flowchart diagram of steps taken to fit the collected data to a Hierarchical Bayesian (HB) model and then, using the model parameters, to construct an Integral Projection Model (IPM).

ysis of IPMs. Traditionally, size-dependent GLM or GLMM vital rate functions for growth, survival, and reproduction—the building blocks of an IPM—are fit independently. Integrating the analyses of multiple vital rates within a single statistical framework allows for direct estimation of temporal or spatial correlations between vital rates based on their joint distribution (Evans et al. 2010, Evans and Holsinger 2012). Failure to account for temporal vital rate correlation can result in misestimation of the stochastic population growth rate and other well-known quantities derived from demographic models (e.g., sensitivities and elasticities; Doak et al. 2005). While Bayesian approaches to estimating vital rate correlation have been used to parameterize a matrix model (Evans et al. 2010), there have been few attempts to combine Bayesian estimation of the joint posterior distribution with an IPM. Furthermore, combining multiple data sets can be a powerful way to indirectly estimate demographic transitions that are difficult to observe (Clark 2003), as we demonstrate below (see The recruitment model).

Third, Bayesian methods provide a powerful way to quantify and propagate uncertainty. The goal of most demographic analyses is to estimate the asymptotic population growth rate (λ in a deterministic environment or λ_S in a stochastic, temporally varying environment), its associated sensitivities or elasticities, and other demographic quantities such as reproductive values, stable state distribution, and generation time; all of these can be viewed as derived quantities of the vital rates. A major challenge in demographic studies is to appropriately model the propagation of uncertainty from the underlying vital rates (the values estimated directly from the data) to the quantities derived from them; again, Bayesian methods are ideally suited for this purpose (e.g., Ghosh et al. 2012, Gelfand et al. 2013). Due to equivariance (any function of a random variable is also a random variable), quantities derived from the posterior are also random variables with associated distributions (Hobbs and Hooten 2015). By using a Bayesian approach, the calculation of the posterior probability distribution of the population growth rate correctly calculates the underlying uncertainty (Ruete et al. 2012). Traditionally, estimates of the confidence interval associated with population growth rates (Caswell 2001), which are based on limit approximations, tend to underestimate uncertainty. Bayesian estimates of the growth rate also provide a direct probability-based measure of the chance that a population will grow or decline. Thus, a Bayesian approach allows for the propagation of uncertainty in estimates of population viability, which is important for deciding on policy or management directions (Merow et al. 2014*a*). Further, the process-related uncertainty in derived quantities such as stochastic population growth rate can be partitioned into ecological sources such as random temporal or spatial effects. By knowing the sources of the variation, ecologists can better understand and predict population dynamics and land managers and other applied practitioners can better devise management strategies.

Fourth, Bayesian methods provide a framework for incorporating prior information about vital rates (e.g., from preliminary studies, other locations, or other related species), which may be particularly valuable when data are scarce. Prior information allows for the quantitative application of previous knowledge rather than simply qualitatively stating in the discussion section whether the current findings are similar to or different from previous studies (Hille Ris Lambers et al. 2005). If no prior information is available, non-informative or vague priors can be seen as a starting point to begin an analysis. Indeed even the notion of a non-informative prior is a misnomer as every prior will contain some information about a parameter or a transformation of a parameter (Hobbs and Hooten 2015). If investigators are uncomfortable choosing a prior, the easiest way to minimize prior influence is to overwhelm the prior with data. However, a Bayesian approach consists of an iterative process such that the well-known saying holds true that "today's posterior becomes tomorrow's prior." Thus, the use of informed priors capitalizes on previous data to estimate a posterior and is a potentially powerful approach to demographic analysis, especially from an adaptive management perspective (Walters 1986, Hobbs et al. 2015).

Finally, from a more philosophical perspective, Bayesian approaches assume that each parameter is a random variable drawn from a distribution. By contrast, frequentist approaches assume that a parameter's value is fixed and the exact estimate becomes better resolved as sample size increases (Walters 1986, Hobbs et al. 2015). In a demographic context, this is the difference between a single value for a vital rate, estimated with increasing precision as sample size increases, and a distribution of uncertainty reflecting the inherent variability of the vital rate (Ellison 2004, Hobbs and Hilborn 2006). The philosophical arguments surrounding Bayesian statistics have been debated elsewhere (e.g., from an ecological perspective, Dennis 1996, Ellison 1996). Here we focus on the practical advantages in demographic contexts, which we suggest are substantial.

While each of these four arguments—modeling process error, combining data sets, propagating uncertainty, and incorporating prior information—could apply in many ecological settings, their combined effect makes Hierarchical Bayesian approaches particularly powerful in the construction and analysis of IPMs. The first three of these four issues will be encountered by every ecologist who undertakes a demographic analysis, and the fourth is one that we suggest more demographers should carefully consider. Having established the "what" and "why" of Bayesian IPMs, we now focus on methodological aspects of how these methods are implemented.

Methods

Integral projection models

Here we provide a brief introduction to IPMs and direct the reader to several recent overview papers for further information (Rees and Ellner 2009, Coulson 2012, Merow et al. 2014*a*, Rees et al. 2014). Since IPMs are an example of an integro-difference equation (IDE), additional reading on Bayesian analysis of IDEs may be helpful (e.g., Wikle 2002, Wikle and Hooten 2010).

The standard, deterministic IPM takes the following form, in which we describe population structure in terms of size (x, y):

$$n(y,t+1)=\int_{L}^{U}[p(x,y)+f(x,y)]n(x,t)dx \quad (2)$$

The variable $n(y, t + 1)$ represents the number of y-sized individuals at time $t + 1$. The abundance of y-sized plants changes from one time step to the next depending on the survival, growth, and reproduction of a population of x-sized individuals over the integral from U to L, which are upper and lower limits, respectively, of possible sizes. There are two paths from size x to y. $p(x, y)$ comprises the survival-growth component of the IPM and can be decomposed into two functions that determine the probability of survival of an x-sized individual, $s(x)$, and the likelihood that the individual will grow from size x to size y over a single time step, $g(x, y)$, such that $p(x, y) = s(x)\, g(x, y)$. The reproductive component, $f(x, y)$, represents the production of individuals of size y from individuals of size x. The specific form of $f(x, y)$ depends upon the organism's life history. For example, $f(x, y)$ may include the number of offspring produced as a function of size, the probability of recruit survival, and the size distribution of surviving recruits. The IPM framework is highly flexible and can easily accommodate additional, discrete demographic states and temporal and spatial environmental variability, as we demonstrate below. Together, the survival–growth and reproduction components form the "kernel" of the IPM, which is a surface of all possible demographic transitions over the course of a single time step.

Bayesian IPM

To demonstrate Bayesian approaches to IPM construction and analysis, we use our demographic studies of the tree cholla cactus, *Opuntia imbricata* [Hawarth] D.C. at the Sevilleta National Wildlife Refuge, a Long-Term Ecological Research (LTER) site in central New Mexico, USA. This long-lived, iteroparous plant is native throughout the Chihuahuan desert and arid grassland habitats of Texas, Oklahoma, New Mexico, and Colorado, USA. Further information about the natural history of the species and study area are provided elsewhere (Miller et al. 2009, Ohm and Miller 2014).

Cholla long-term demographic data

Most of the demographic data (the "long-term" data) came from 10 years (2004–2014) of longitudinal observations of 798 censused plants in three groups of plants that were distributed across multiple plots or spatial blocks. The first group consisted of 134 naturally occurring plants distributed over four spatial blocks that were censused from 2004 to 2008 (these were the high elevation control plants described in [Miller et al. 2009, Ohm and Miller 2014]). A second group of 517 naturally occurring plants distributed over six 30 × 30 m plots was censused from 2009 to 2014; an additional 147 plants in two additional plots were added to this census from 2011 onward. These eight plots were searched each year, and new recruits were added to the census as they were detected. The third group of observations came from seed addition experiments described below. In late May/early June of each year, we recorded for each plant: survival, three size measurements (height [cm], maximum crown width [cm], and crown width perpendicular to the maximum [cm]), and number of flower buds. Size measurements were converted to the volume of a cone (cm^3), where length was plant height and radius was 0.5 × the mean of the maximum and perpendicular crown widths. In total, the data set included 2732 observed inter-annual transitions spanning the tree cholla size distribution.

Seed addition experiment

To estimate germination, recruitment, and growth/survival of new recruits, known quantities of seeds were added to 0.25 × 0.25 m plots in January 2004. These plots were revisited in September of 2004 and 2005, after germination was triggered by monsoon precipitation, at which time recruits were counted and tagged and their sizes recorded as above. New recruits were censused again in May 2005 and 2006, to estimate survival from late summer germination until the regular spring census period. Further details of field methods are provided in Miller et al. (2009). Because seed maturation and dispersal happen in fall and winter and because late-summer monsoons are a key driver of germination, a seed initiated in May of year t would be detected as a new recruit not in May of $t + 1$ but more likely May of $t + 2$, at the earliest. Thus, there is a 1-year time lag in the regeneration phase of the life cycle. In addition, we observed new recruits in seed addition plots in September 2005 and none in control (no seed) plots, indicating potential for at least a 2-year seed bank (recruits detected in May of $t + 3$). The age-structured seed bank will introduce discrete states to the cholla IPM (see below).

IPM structure

The tree cholla IPM consists of continuously size-structured plants ($N(x, t)$) plus two discrete seed states to capture recruitment in years $t + 2$ and $t + 3$ from

seed production in year t. Because the long-term demographic data included random temporal and spatial heterogeneity (repeated observations across years and plots), our IPM is temporally and spatially stochastic (Rees and Ellner 2009). Dynamics of the 1-year-old (yo) and 2-yo seed banks (B_1 and B_2, respectively) in plot p and year t are given by:

$$B_1(p,t+1) = s\delta \int_L^U P_{Fl}(x,\boldsymbol{\theta}(t),\boldsymbol{\kappa}(p))\, F(x,\boldsymbol{\theta}(t),\boldsymbol{\kappa}(p))\, N(x,p,t)\, dx, \quad (3)$$

$$B_2(p,t+1) = (1-g_1)\, B_1(p,t) \quad (4)$$

The functions $P_{Fl}(x)$ and $F(x)$ give the probability of flowering and number of flowers produced, respectively, for an x-sized plant. The vectors $\theta(t)$ and $\kappa(p)$ contain random deviates representing temporal and spatial variability, respectively. The integral is multiplied by the number of seeds per fruit (s) and probability of transitioning from the plant to the seedbank (δ) to give the number of seeds that enter the 1-yo seed bank. After the late-summer monsoon rains, plants recruit out of the 1-yo seed banks with probability g_1 or transition to the 2-yo seed bank with probability $(1-g_1)$. Seeds in the 2-yo seed bank are assumed to either germinate (probability g_2) or die.

Continuous-size dynamics are given by:

$$N(y,p,t+1) = (g_1 B_1(p,t) + g_2 B_2(p,t))\eta(y)\phi + \int_L^U S(x,\boldsymbol{\theta}(t),\boldsymbol{\kappa}(p))G(y,x,\boldsymbol{\theta}(t),\boldsymbol{\kappa}(p))N(x,p,t)dx. \quad (5)$$

The first term indicates recruitment from the seed banks to size y, where $\eta(y) \sim N(\mu_R, \sigma_R)$ and μ_R and σ_R are the mean and standard deviation, respectively, of the size distribution of new recruits at the time of the census. Mortality between late summer germination and the May census is accounted for with survival probability φ. The second term reflects growth from size x to y ($G(y, x)$), conditioned on the probability of survival at size x ($S(x)$) and integrated over all sizes. Future size y follows a Gaussian distribution where mean $\mu_G(x)$ is the expected future size of an x-sized plant and σ_G is the standard deviation of the residual variance about the growth function. As above, $\theta(t)$ and $\kappa(p)$ incorporate process noise from spatial and temporal variability. These random effects only appear in the vital rates estimated from long-term data; we were unable to model process noise in the parameters derived from short-term studies, such as germination and seedling survival.

Bayesian parameter estimation

The vital rate model.—The long-term data were used to estimate the posterior density of four potentially co-varying IPM vital rates (growth, survival, probability of flowering, and the number of flowers produced), which we modeled as functions of size. Throughout the text, we will refer to the model described below and outlined in Fig. 2 as the "vital rate model." The biological sources of variance (process error) in the long-term vital rate data include individual heterogeneity, plot/spatial block, and year, all of which could be modeled in a single hierarchical Bayesian (HB) framework. We illustrate the approach by modeling random plot-to-plot and year-to-year variance, including potential for vital rate correlations across years. For instance, a good year for growth would also be a good year for any vital rate that was positively correlated with growth. Numerous examples in the literature show the importance of accounting for the correlation between vital rates when estimating population growth trajectories (e.g., Doak 1995, Morris and Doak 2002, Evans et al. 2010).

To account for temporal correlation between vital rates, we adopted an approach ("hierarchical centering") used in a matrix model by Evans et al. (2010) whereby each of the individual vital rates is linked by a "model-wide" effect of year (Fig. 2). Other methods can be used to estimate the correlation matrix and the corresponding covariance matrix associated with vital rates such as directly estimating the covariance matrix or using the scaled inverse-Wishart (Clark 2007, Gelman and Hill 2007, Kéry and Schaub 2012). These methods can become quite complicated as the dimensions of the covariance matrix increase and may lead to a mis-estimation of the correlation coefficients when they occur at the extremes of [−1, +1] (Gelman 2006, Huang and Wand 2013). Given the above, we decided to incorporate a "model-wide" approach of Evans et al. (2010) into our hierarchical model. To assess potential for spatial correlations in the vital rate data (e.g., plots that are good for growth are also good for survival), we examined the correlogram of the residuals of the spatio-temporal model described below for eight georeferenced plots. We found no spatial pattern and the 95% credible intervals (CIs) for each spatial lag overlapped the expected value for Moran's I given complete randomization (Cressie 1993, Dantin and Fortin 2014). This was not surprising given that the plots were relatively close together (mean distance = 200 m, SD = 138 m). We therefore model spatial variance independently for each vital rate. However, for other studies where correlation exists between sites, modeling spatial correlation is possible.

We estimated the parameters associated with growth, survival, probability of flowering, and the number of flowers produced from a connected suite of hierarchical models (Fig. 2). Here we illustrate our approach with the growth sub-model. The associated details regarding the three other vital rates correlated with growth are quite similar and are provided in the Appendix.

For growth, we modeled the natural log of future size (volume) $y^G_{i,p,yr+1}$ of individual i, in plot p, in year $yr + 1$ given its current log size $x_{i,p,yr}$ as:

$$y^G_{i,p,yr+1} \sim N\left(\mu^G_{i,p,yr+1}, \sigma^G\right), \quad (6)$$

$$\mu^G_{i,p,yr+1} = \alpha^G_{yr} + \beta^G x_{i,p,yr} + \gamma^G \varepsilon_{yr} + \xi^G_p,$$

$$\alpha^G_{yr} \sim N\left(\mu^G_\alpha, \sigma^G_\alpha\right),$$

$$\varepsilon_{yr} \sim N(0, \sigma_{\omega}),$$
$$\gamma^{G} = 2\Xi^{G} - 1,$$
$$\Xi^{G} \sim \text{Bernoulli}(\pi^{G}),$$
$$\xi_{p}^{G} \sim N\left(0, \sigma_{\xi}^{G}\right).$$

Here, $y_{i,p,yr+1}^{G}$ has a mean $\mu_{i,p,yr+1}^{G}$ and standard deviation σ^{G}. The mixed-effects linear relationship of future size to current size, $x_{i,p,yr}$, consists of a random intercept, α_{yr}^{G}, that varies by year, a fixed slope of β^{G}, a model-wide effect, ε_{yr} which connects each of the vital rates that co-vary (Fig. 2), the response of growth to year effects γ^{G}, and the variability between plots or spatial blocks, ξ_{p}^{G}. The random intercept, which accounts for the year-to-year variability associated with growth, has a mean μ_{α}^{G} and standard deviation σ_{α}^{G}. We also considered models that allowed for temporal variability in both the intercept and slope β^{G}. However, these models failed to converge (see below for definition), perhaps due to lack of parameter identifiability (Kéry 2010). The model-wide year effect, ε_{yr}, has a mean of 0 and a standard deviation of σ_{ω}. The growth response to year effects, γ^{G}, can only take on values of −1 and +1 and determines whether the model-wide year effect is positively or negatively correlated with an arbitrarily assigned vital rate (Evans et al. 2010, Evans and Holsinger 2012). The vital rate chosen has no effect on the correlation or covariance structure (Doak et al. 1994). For the long-term demographic data, we set $\gamma = 1$ for the number of flowers produced and allowed γ to vary for the other three vital rates based on a Bernoulli random variable, which for growth is Ξ^{G}. Spatial variability associated with plot or spatial block has a mean of zero and a standard deviation of σ_{ξ}^{G}. We used vague prior distributions (Table 1) for each of the parameters above.

The Bayesian posterior (Eq. 1) given the above becomes:

$$P(\alpha_{yr}^{G}, \beta^{G}, \Xi_{p}^{G}, \sigma^{G}, \Xi^{G}, \varepsilon_{yr}, \sigma_{\omega}, \sigma_{\xi}^{G}, \pi^{G}, \mu_{\alpha}^{G}, \sigma_{\alpha}^{G} | \mathbf{Y^{G}}) \propto$$
$$\overbrace{\prod_{i=1}^{n_G} \prod_{p=1}^{P} \prod_{yr=1}^{\text{YR}-1} N\left(y_{i,p,yr+1}^{G} | \alpha_{yr}^{G} + \beta^{G} x_{i,p,yr} + \gamma^{G} \epsilon_{yr} + \xi_{p}^{G}, \sigma^{G}\right)}^{\text{Likelihood}}$$
$$\overbrace{\times \prod_{yr=1}^{\text{YR}} N\left(\alpha_{yr}^{G} | \mu_{\alpha}^{G}, \sigma_{\alpha}^{G}\right) \prod_{yr=1}^{\text{YR}} N\left(\varepsilon_{yr} | 0, \sigma_{\omega}\right) \prod_{p=1}^{P} N\left(\xi_{p}^{G} | 0, \sigma_{\xi}^{G}\right)}^{\text{Priors}} \quad (7)$$
$$\overbrace{\times \textit{Bernoulli}\left(\Xi^{G} | \pi^{G}\right) N(\beta^{G} | 0, 10^{3})}^{\text{Priors(cont.)}}$$
$$\overbrace{\times N(\mu_{\alpha}^{G} | 0, 10^{3}) N(\sigma_{\alpha}^{G} | 0, 10) U\left(\sigma^{G} | 0, 10^{3}\right) U\left(\sigma_{\omega} | 0, 10\right) U\left(\sigma_{\xi}^{G} | 0, 10^{3}\right) U\left(\pi^{G} | 0, 1\right).}^{\text{Hyperpriors}}$$

Here n_G is the number of individuals measured in a plot each year, YR is the number of years measured, and P is the number of plots. The future size of the plants given their current size is represented by the data vector $\mathbf{Y^{G}}$.

The recruitment model.—The vital rate model described above does not capture the regeneration process. As in many other demographic studies, regeneration and recruitment are the least understood transitions of the cholla life cycle. In particular, we have little direct information on the dispersal of seeds from maternal plants to the seed bank (probability δ in Eq. 3). Here we highlight how Bayesian methods allow us to combine information from multiple data sets to draw an indirect inference for this latent (unobserved) parameter; we refer to this estimation process as the "recruitment model". We also use the recruitment model to demonstrate the application of an informed prior based on preliminary data.

The recruitment model combines field and experimental data to estimate the number of recruits observed in the cholla census plots during 2014. Given what we know about seed banking in this species, new recruits detected in 2014 must reflect a combination of recruitment from the 1-yo seed bank (seeds produced in 2012, banked in 2013, detected as recruits in 2014) and recruitment from the 2-year-old seed bank (seeds produced in 2011, banked in 2012, still banked in 2013, detected as recruits in 2014). Our recruitment model takes independent data on the total number of seeds produced in 2011 and 2012 (from the demography census) and the germination probabilities of seeds in the 1- and 2-yo banks (from the seed addition experiment) to generate an indirect inference for the probability that seeds transition to the seed bank (δ). Thus, even though we do not directly measure this probability or observe it, we can still estimate this latent variable using inference gained from combining multiple data sets. We were limited to using 2014 recruitment data because it was the first year for which we were confident in our seedling search process. We therefore assume that the seed banking probability does not vary through time. Because the seed addition experiment was a

short-term study, we additionally assume that germination probabilities do not vary through time.

The recruitment model takes the form:

$$\begin{gathered} y_{t,p}^{R1} \sim Binomial\left(\delta g_1, y_{t-2,p}^{F} s\right), \\ y_{t,p}^{R2} \sim Binomial\left(\delta\left(1-g_1\right) g_2, y_{t-3,p}^{F} s\right) \\ y_{t,p}^{R} = y_{t,p}^{R1} + y_{t,p}^{R2}, \\ \text{logit}\left(\delta\right) = \alpha^{\delta}, \\ y_i^{g1} \sim Bernoulli\left(g_1\right),\ y_i^{g2} \sim Bernoulli\left(g_2\right), \\ \text{logit}\left(g_1\right) = \alpha^{g_1},\ \text{logit}\left(g_2\right) = \alpha^{g_2}, \\ y_i^{s} \sim Poisson\left(s\right). \end{gathered} \tag{8}$$

The total number of new recruits $y_{t,p}^{R}$ in plot p at time t is the sum of two cohorts. The first cohort ($y_{t,p}^{R1}$) is a product of two binomial processes (the probability of transitioning from the plant to the seed bank, δ, and germinating, g_1), where the number of trials is total seed production in plot p, year $t-2$ (seed production is the product of the total number of fruits over all plants in the plot, $y_{t-2,p}^{F}$, and the number of seeds per fruit, s). The second cohort ($y_{t,p}^{R2}$) is estimated similarly but is conditional on the probability of not germinating from the 1-yo bank. For each of the random variables, we used standard distributions given the data of the number of seeds germinating in year one, y_i^{g1}, seeds germinating in year two, y_i^{g2}, the number of fruits produced, $y_{t,p}^{F}$, and the number of seeds per fruit, y_i^{s}.

As pointed out earlier, the use of informed priors represents a distinct advantage of Bayesian analysis since it allows for the combination of previous knowledge with newly collected data (Clark 2007, King et al. 2010, Hobbs and Hooten 2015). We used surveys of fruits on the ground beneath maternal plants as a starting point for estimating the effective seed dispersal parameter, δ. Once ripe and dry, cholla fruits fall to the ground beneath maternal plants, where rodents consume the seeds. We collected observations of the proportions of total fruits produced by 24 plants that were subsequently detected beneath the plants and remained intact (Miller et al. 2009). These data provide a rough approximation of the plant-to-seed bank transition rate and were therefore used to generate an informative prior. We modeled the fruit census data as:

$$\begin{gathered} y_i^{\delta_c} \sim Bernoulli\left(\delta_c\right), \\ \text{logit}\left(\delta_c\right) = \alpha^{\delta_c}. \end{gathered} \tag{9}$$

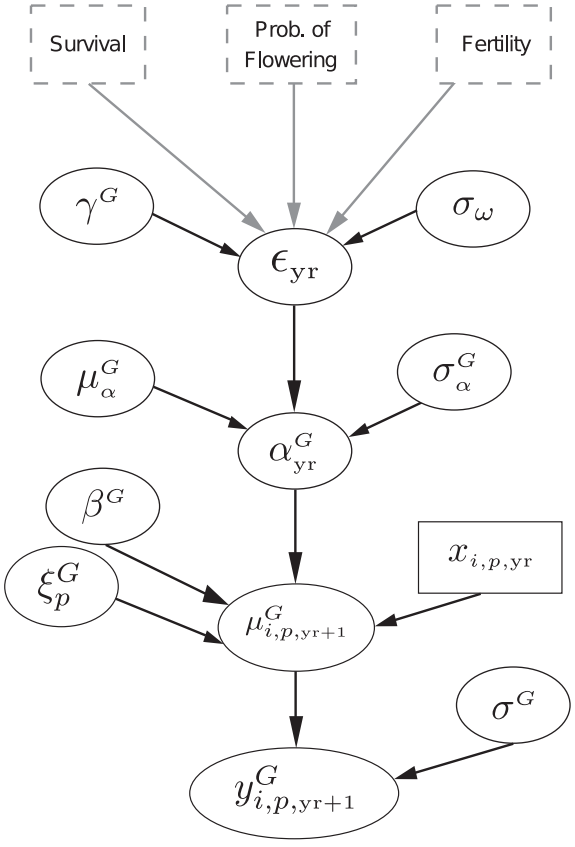

FIG. 2. Directed Acyclic Graph (DAG) for the Bayesian hierarchical model for growth between years that accounts for spatial variability between plots and allows for temporal correlation between cholla life history events. Circles represent distributions and solid boxes represent data. Dashed boxes represent the three other associated vital data, which are not fully represented here (see Appendix). Parameters are defined in Table 1 and the text.

Whether a fruit $y_i^{\delta_c}$ remains beneath a plant is a Bernoulli random variable given the probability δ_c. We used the corresponding median and 95% CI of α^{δ_c} from Eq. 9 (Table 1) to construct an informed prior for δ (Median = 3.0% with a 95% CI that ranged from 1.76% to 4.77%) in the full recruitment model.

The resulting posterior distribution given the above model is:

Here $f(\alpha^{g_1})$ and $h(\alpha^{g_2})$ represent functions of the intercept values associated with germination. Although we do not directly estimate δ, we are able to estimate its value

$$\begin{gathered} P\left(\alpha^{\delta}, \alpha^{g_1}, \alpha^{g_2}, s \mid Y^{g1}, Y^{g2}, Y_2^F, Y_3^F, Y^s, Y^R\right) \propto \\ \prod_{i=1}^{N_1} Bernoulli(y_i^{g1} \mid f(\alpha^{g_1})) \prod_{n_2=1}^{N_2} Bernoulli(y_i^{g2} \mid h(\alpha^{g_2})) \prod_{i=1}^{I} Poisson\left(y_i^{s} \mid s\right) \\ \times \prod_{p=1}^{P} \left[Binomial\left(y_p^{R1}, y_{t-2,p}^{F} \mid s, \delta, g_1\right) + Binomial\left(y_p^{R2}, y_{t-3,p}^{F} \mid s, \delta, g_1, g_2\right) \right] \\ \times N\left(\alpha^{\delta} \mid -3.48, 0.300\right) N\left(\alpha^{g_1} \mid 0, 10^3\right) N\left(\alpha^{g_2} \mid 0, 10^3\right) N(s \mid 0, 10^3). \end{gathered} \tag{10}$$

TABLE 1. Median and 95% credible intervals (CIs) for the parameters used to construct the integral projection matrix.

Parameter	Median (95% CI)	Prior distribution
1-year germination intercept, α^{g_1}	−5.12 (−5.348, −4.908)	N(0, 1000)
2-year germination intercept, α^{g_2}	−5.46 (−5.742, −5.200)	N(0, 1000)
Precensus intercept, α^{ϕ}	−1.66 (−2.343, −1.065)	N(0, 1000)
Plant-to-seedbank intercept, α^{δ}		
Informed prior	−3.09 (−3.467, −2.729)	N(−3.48, 3.33)
Uninformed prior	−3.04 (−3.436,−2.656)	N(0, 1000)
Mean seeds per fruit, s	125 (122.9, 127.9)	U(0, 500)
Mean size of new recruit, μ_R	3.251 (−3.674, −2.835)	U(−50, 50)
SD of new recruit size, σ_R	0.74 (0.517, 1.192)	U(0, 100)
Mean survival intercept, μ_α^S	0.55 (−0.307, 1.578)	N(0, 1000)
SD of survival intercept, σ_α^S	0.92 (0.478, 2.148)	U(0, 10)
Survival slope, β^S	0.36 (0.310, 0.420)	N(0, 1000)
Spatial SD for survival, σ_ξ^S	0.17 (0.006, 0.596)	U(0, 1000)
Mean growth intercept, μ_α^G	0.87 (0.585, 1.142)	N(0, 1000)
SD of growth intercept, σ_α^G	0.18 (0.009, 0.495)	U(0, 10)
Growth slope, β^G	0.91 (0.899, 0.924)	N(0, 1000)
Spatial SD for growth, σ_ξ^G	0.06 (0.015, 0.133)	U(0, 1000)
SD of growth, σ^G	0.85 (0.825, 0.868)	U(0, 1000)
Mean probability of flowering intercept, $\mu_\alpha^{P_{Fl}}$	−20.21 (−22.473, −17.876)	N(0, 1000)
SD of probability of flowering intercept, $\sigma_\alpha^{P_{Fl}}$	1.67 (0.980, 0.495)	U(0, 10)
Probability of flowering slope, $\beta^{P_{Fl}}$	1.81 (1.636, 1.978)	N(0, 1000)
Spatial SD for probability of flowering, $\sigma_\xi^{P_{Fl}}$	0.41 (0.209, 0.807)	U(0, 1000)
Flowers produced intercept, μ_α^F	−6.02 (−7.006, −5.023)	N(0, 1000)
SD of flower intercept, σ_α^F	0.27 (0.030, 0.689)	U(0, 10)
Flowers produced slope, β^F	0.68 (0.597, 0.757)	N(0, 1000)
Spatial SD for flowers produced, σ_ξ^F	0.25 (0.140, 0.469)	U(0, 1000)
SD of flowers produced, σ^F	0.85 (0.793, 0.903)	U(0, 10)
Model-wide year effect, σ_ω	0.241 (0.028, 0.559)	U(0, 1)

Note: The last column contains the prior distribution for each of the parameters.

indirectly given the informed prior and the other related demographic data collected.

Other parameters.—Two additional parameters were estimated separately: new recruit size and precensus recruit survival. The data were collected as part of a 2005–2006 census of recruits. Full details of the associated models are presented in the Appendix.

Defining priors.—To start a Bayesian analysis, we need to first choose a prior distribution for each parameter (Fig. 1). Lacking relevant prior information, we chose "flat" or "vague" priors (uniform or normal distributions with large variance) for most of the estimated parameters. To gauge the impact of an informative prior on the posterior, it is common to conduct a prior sensitivity analysis where different sets of priors are used and the resulting posteriors are compared (Gelman et al. 2003, Elderd et al. 2013). For the vital rate model, we used only vague priors and, thus, did not conduct a sensitivity analysis. However, the recruitment model contained an informed prior (for δ). Thus, we conducted a prior sensitivity analysis to determine the prior's influence on the posterior estimates of the model.

Assessing model convergence and fit.—To obtain posterior estimates of the demographic parameters, we fit models using Markov chain Monte Carlo (MCMC) simulations via JAGS, a popular and freely available Bayesian software package (Fig. 1). For each model,

we obtained three separate chains, each for 18 000 iterations. The initial conditions for each chain were randomly chosen. The first 5000 iterations were discarded as burn-in to eliminate any transients associated with the initial conditions. All other iterations were retained to estimate the associated posterior distribution. We did not thin the chains (i.e., keep every m^{th} iteration of the chain), which is routinely done in ecology (Link and Eaton 2012). Link and Eaton (2012) show that thinning is inefficient and reduces the precision of the MCMC-based estimates. Others have also argued that all samples from the MCMC chain contain information about the parameter and, thus, all samples should be retained (King et al. 2010).

We assessed MCMC convergence using standard metrics to examine both within-chain and between-chain convergence. First, we calculated the Brooks-Gelman-Rubin statistic or $\hat{R}$, which compares within- and between-chain variation (Brooks and Gelman 1998). Values close to 1 indicate good between-chain convergence and values greater than 1.1 suggest convergence problems (Gelman and Hill 2007). We also used the Heidelberger-Welch diagnostic, which assesses convergence of each chain by testing for stationarity (Heidelberger and Welch 1983). The test is one of many available in the R coda package (Plummer et al. 2006). Specifically, the Heidelberger-Welch diagnostic tests whether or not the sample chain is stationary such that the within-in chain's mean does not change over the MCMC sample. After discarding the burn-in iterations and assessing convergence, all chains were combined and visually inspected before proceeding.

To assess overall model fit to the data, we carried out posterior predictive checks (Gelman et al. 1996, Gelman and Hill 2007, Kéry 2010). Posterior predictive checks use a standard discrepancy statistic, such as the sum of squared deviations of observed values from predictions, to examine how well the fitted model can generate data that are similar to the actual data. The simulated data and the actual data are compared by measuring the lack of fit of both data sets to model predictions (Gelman and Hill 2007, Kéry 2010). Large differences in the lack of fit between the two data sets indicate that the model misfits the actual data and the model may need to be modified (Fig. 1). Lack of fit can be examined visually or be used to compute a Bayesian *P*-value, which quantifies the frequency with which the discrepancy for the simulated data is greater than the discrepancy for the actual data. Values near 0.5 indicate that the model does a good job of fitting the data (Kéry 2010).

Bayesian model selection.—To determine if the model that included temporal correlations and spatial heterogeneity best fits the data, we also fit three additional, simpler models that lacked explicit vital rate correlation, plot variance, or both (Table 2). We used K-fold cross validation, where K = 10, to evaluate the models (Hooten and Hobbs 2015). K-fold cross-validation consists of dividing up the data set into K smaller sub-sets. One sub-set is left out, $\boldsymbol{Y}_k$, and the rest of the data, $\boldsymbol{Y}_{-k}$, are used to train the model. The parameters derived from the model using the training data set, $\boldsymbol{Y}_{-k}$, are used to predict the responses of the $\boldsymbol{Y}_k$ subset or the test data. Each of the m iterations of the posterior estimates of the model's parameters, $\boldsymbol{\Theta}^{(m)}$ is used to compute the cross-validation score, calculated as:

$$\mathrm{kCV} = -2\sum_{k=1}^{K}\log\left(\frac{\sum_{m=1}^{M} P(Y_k \mid Y_{-k}, \boldsymbol{\Theta}^{(m)})}{M}\right). \quad (11)$$

We multiplied the standard score by −2 so that the model with the lowest score corresponds to the model that best fits the data as is standard for other traditional model selection metrics such as Akaike information criterion, AIC, or Deviance information criterion, DIC (following the convention of Hooten and Hobbs 2015). Cross-validation will tend to reject complicated models given that these tend to score poorly when predicting beyond the data used for fitting (Cressie et al. 2009). We did not use the more well-known metrics such as DIC or Watanabe-Akaike information criterion, WAIC, since these model selection criteria are not suitable for mixture models (i.e., models arising from a mixture of distributions such as multiple normal processes) or models with spatial or temporally correlated data, respectively (Gelman et al. 2014, Hooten and Hobbs 2015). Additionally, DIC tends to select overly complicated models and is not recommended for hierarchical models (Hooten and Hobbs 2015).

All of the models were coded in R (R Core Team 2013) and the MCMC chains were obtained using JAGS and the R2JAGS package (Su and Yajima 2014). Data and code for the vital rate and the recruitment model are included in the Supplemental Information.

Building the IPM from the vital rates

Analyzing an IPM generally requires that the projection integral be discretized into an approximating matrix (Ellner and Rees 2006). The dimensions of the matrix and the behavior of the model near its size boundaries

TABLE 2. Model comparison using *K*-fold cross validation (K = 10) scores for the hierarchical vital rate models of the cholla long-term demographic data (survival, growth, probability of flowering, and fecundity).

Model	Cross-validation score
No correlation and no spatial heterogeneity	17 184.4
Correlation and no spatial heterogeneity	17 123.6
No correlation and spatial heterogeneity	17 180.8
Correlation and spatial heterogeneity	17 121.0

Note: Note that the lowest score denotes the model that best fits the data (Eq. 11).

are topics that warrant careful consideration and have been discussed elsewhere (Williams et al. 2012). We analyzed the tree cholla model with an approximating matrix of size 200 × 200. We set the lower and upper bounds of the continuous size distribution to 10% less than and greater than the observed minimum and maximum, respectively.

The stochastic population growth rate λ_S and the vital rate sensitivities were derived from the posterior of the parameter estimates. The stochastic population growth λ_S rate is given by the long-run geometric mean of annual growth rates (Caswell 2001, Rees and Ellner 2009):

$$\log(\lambda_S) = E\left[\log\left(\frac{N_{t+1}}{N_t}\right)\right] \quad (12)$$

where N_t is the total population size and E represents the expected value. This quantity has an analytical approximation (Tuljapurkar 1982) but many demographic studies rely on numerical simulation, as we do here. See Rees and Ellner (2009) for further guidance on estimating λ_S from stochastic IPMs. To calculate the posterior distribution of λ_S, we drew 500 sets of values from the posterior distribution of the vital rate coefficients (Table 1, Fig. 1). For each parameter set, we simulated population dynamics (Eqs 3–5) for 5000 yrs and took the geometric mean growth rate of the latter 4500 yrs (discarding the first 10% as transient dynamics). For a single parameter set, the IPM kernel varied from year to year based on random draws from the distributions of temporal variance, and from plot to plot based on random draws of plot variance (Eqs 3–5). The distribution of λ_S across parameter sets therefore reflects the total uncertainty in the population growth rate, including estimation error of the vital rate coefficients and two types of process error: plot-to-plot and year-to-year variance in demography, including vital rate correlations across years (year-to-year variance is implicit in λ_S, the growth rate for populations in temporally variable environments). As a prior sensitivity analysis, we compared the posterior probability distributions for δ and λ_S using the vague and informed priors for the plant-to-seed bank transition probability. We also compared λ_S between the alternative candidate models fit to the vital rate data (Table 2) to assess how accounting for vital rate correlations and spatial variance affected the predictions of the IPM.

Perturbation analysis of IPM parameters

Prospective perturbation analysis of IPMs can be important for predicting population responses to environmental change (Williams et al. 2015) and human intervention (Wallace et al. 2013), or for inferring the direction and strength of natural selection on demographic rates (Childs et al. 2011, Coulson 2012). There are at least three types of perturbation (sensitivity or elasticity) analyses that could be conducted with an IPM: perturbation of the kernel values, the vital rate coefficients, or the means of the vital rate functions (Rees and Ellner 2009). For populations in temporally varying environments, such as ours, sensitivities and elasticities of the population growth rate to temporal variance in kernel values or vital rate coefficients can also be calculated (Rees and Ellner 2009). As with the population growth rate, the joint posterior distribution of the demographic parameters can be used to quantify uncertainty in any of these quantities. We calculated the posterior distributions of the sensitivities of λ_S to the vital rate coefficients ($\partial \lambda_S / \partial \theta_i$), including the intercepts and slopes of the size-dependent functions (Table 1). For each parameter, we calculated sensitivities of λ_S to the parameter for each of 500 draws from the joint posterior distribution. Sensitivity calculations were based on the analytical approximations of Rees and Ellner (2009). Code for all IPM construction and analysis is provided in the Appendix.

Results

Bayesian model selection, diagnostics, and parameter estimates

The cross-validation scores for the model that considered temporally correlated parameter values and spatial heterogeneity received the most support from the data compared to the alternative models (Table 2). However, the second-ranked model that contained temporally correlated parameters but no spatial variance had a cross-validation score close to the best fit model. All diagnostic tests indicated that both models fit the data well. For the spatio-temporal model, the trace plots showed that the Markov chains converged to the same area of parameter space (Fig. 3A shows one example for the slope of the growth function, β^G; see also the Appendix). Additionally, all values of $\hat{R}$ were less than 1.1 (Fig. 3B) and each of the chains passed the stationarity tested posed by the Heidelberger-Welch diagnostic, further indicating that all of the Markov chains converged. The posterior predictive checks and Bayesian *P*-values also showed that the best fit and the second best fit model provided a good fit to the data. Fig. 4 shows an example of a predictive check for the growth sub-model (Eq. 6) and other metrics indicating that the growth data met the assumption of normally distributed residuals with constant variance.

When considering the influence of an informed prior, we directly examined the effects of the prior on the probability of a seed transitioning into the seed bank, δ. The estimates were not appreciably different if we used a vague prior vs. an informed prior (Fig. 5, Table 2), though there was a slight shift of the posterior toward the informed prior (lower seed transition probability), which is to be expected. Overall, the likelihood dominated the posterior for the plant-to-seed bank transition rate.

Given the above model diagnostics and model comparison results, the combined chains were used to calculate parameter estimates associated with the IPM (Table 1) and compare the models to the data (Figs. 6 and A2).

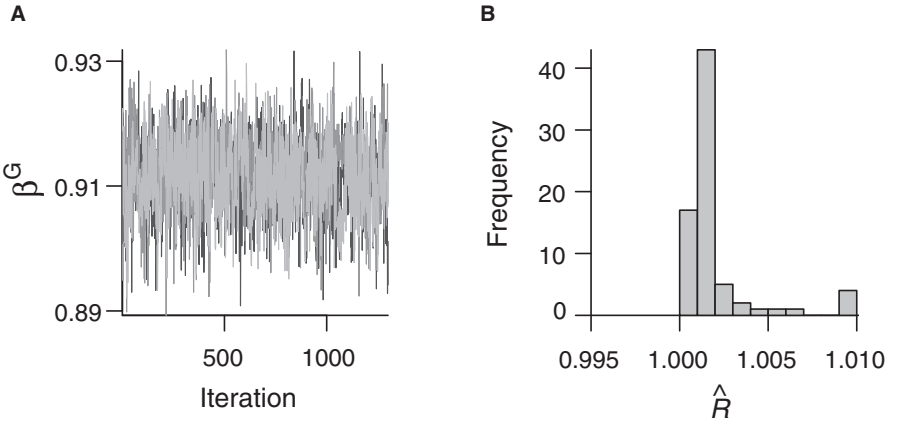

FIG. 3. (A) A trace plot for the slope of the growth model (β^G), a representative parameter (the other parameters showed similar patterns). The trace plot shows that all three chains, represented by different shades of gray, overlap considerably. A subset of the chains is plotted (≈10%) for ease of graphical presentation. (B) Distribution of values of the Brooks-Gelman-Rubin ($\hat{R}$) statistic for convergence of the MCMC chains across all parameters. $\hat{R}$ values less than 1.1 indicate parameter convergence. Given the above and other diagnostics (e.g., Heildelberger-Welch), we conclude that the chains have converged and that the samples are independent draws from the distribution of β^G.

Fig. 6 shows the 95% prediction interval (PI) for each of the vital rates. The PI forecasts the distribution of future observations of a vital rate, accounting for its expected value and variance. By contrast, the 95% CI, shown in Fig. A2, encompasses the uncertainty associated only with the mean estimate of the vital rate, and is therefore narrower than the PI. As shown in Figs. 6 and A2, the best fit model does a good job of fitting the data, although there were a few individual transitions or probabilities that occurred outside the prediction interval envelope, particularly for growth (Fig. 6B). These potential outliers could represent measurement error or the extremes of individual variation.

IPM results

The posterior probability distribution for the stochastic population growth rate (λ_s), accounting for all sources of uncertainty in the demographic data, indicated that the tree cholla population is predicted to decline (Fig. 7). The informed prior for the plant-to-seed bank transition rate had virtually no influence on the stochastic growth rate. Mean λ_s was 0.96, suggesting that, on average, the population is expected to shrink by 4% per year. The 95% CI and almost the entirety of the posterior distribution fell below 1.0; thus, the probability that this population is stable or growing is virtually zero. The posterior distribution of stochastic growth rates predicted by the best fit vital rate model (Table 2) was very similar to the distribution predicted by simpler but poorer fitting models that did not explicitly account for spatial variance or vital rate correlations (Fig. 7B). Accounting for spatial variance widened the posterior distribution of λ_s, increasing uncertainty. Also, accounting for vital rate correlation tightened the distribution, reducing uncertainty. These effects, however, were very slight. Overall, the results give the qualitative impression that the best fitting vital rate model generated predictions that are nearly identical to those of poorer fitting models. The results further suggest that most of the uncertainty in λ_s stems from estimation error and not process variability, since turning "off" spatial heterogeneity had virtually no effect.

The posterior distributions of the sensitivities of λ_s to the vital rates are shown in (Fig. 8). Parameters governing size-dependent growth and survival, and particularly the slope of the relationship between current and future size (β^G), dominated the sensitivities (Fig. 8A). All parameters related to regeneration, including flowering, seed production, seed survival, and germination, affected population growth very weakly (note scales of Figs. 8A and 8B). The parameter for the plant-to-seed bank transition (δ) was among these, explaining why its prior had no influence on the population growth rate. Among the parameters of the recruitment model, λ_s was most responsive to the slope of the flowering function, which controls how steeply the probability of flowering increases with size (Fig. 6C). Vital rate sensitivities were generally negatively correlated with their spatial and temporal variances such that higher-sensitivity vital rates exhibited lower variability (Fig. 9). For most vital rates, temporal variability exceeded spatial variability. Fertility was the exception with equal spatial and temporal variability.

DISCUSSION

Our results suggest that hierarchical Bayesian approaches are both a viable and valuable method for parameterizing IPM models. Specifically, our models, implemented with freely available software packages, accurately described growth, survival, and fecundity for a long-lived species

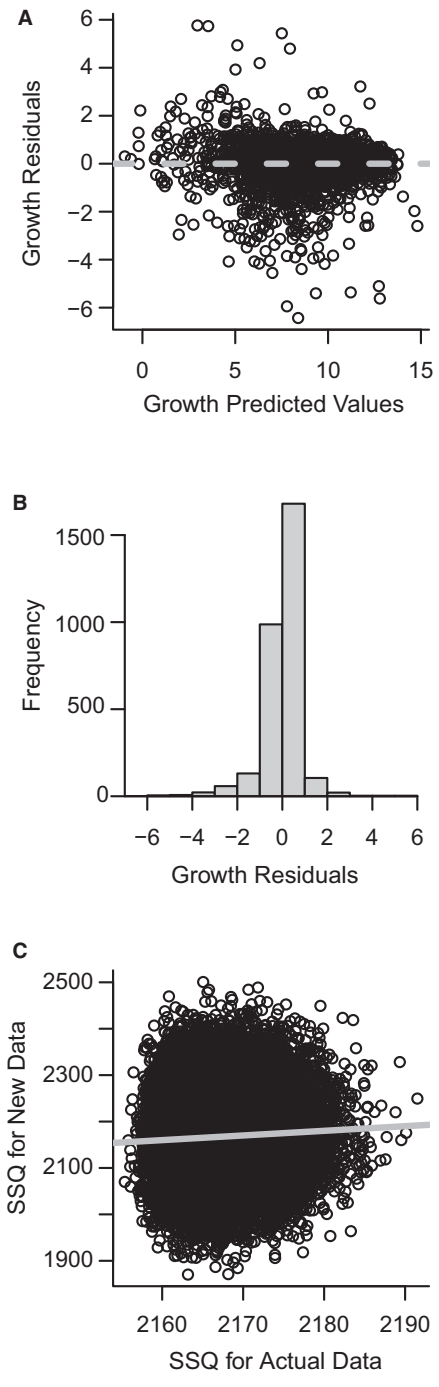

FIG. 4. Posterior predictive check of the growth estimates where (A) the growth residuals and the predicted values do not show a pattern indicating a good fit of the model to the data. This is further confirmed by (B) the centering of the residual histogram and (C) the sum of squares (SSQ) comparison between the actual data given the model fit and new data generated from the model. Gray line in (C) is 1:1. The Bayesian *P*-value for the SSQ plot equals 0.52. The fit for the other variables in the model is comparable.

with a complex life history, including process variability stemming from unmeasured factors that vary across years and plots. Once integrated into IPMs, these vital rate models allowed us to estimate demographic quantities, such as λ_s and their sensitivities to the vital rate parameters, of great interest for both basic and applied reasons. Through their reliance on GLMs or GLMMs, IPMs have a natural interface with hierarchical Bayesian methods of statistical modeling. Exploring and exploiting this interface, as we have done with the cholla case study, reveals several advantages, including the ability to: incorporate data from multiple studies to infer unobservable processes; accommodate complex variance and covariance structures; incorporate prior information about poorly known demographic transitions; parse out the uncertainty associated with process and measurement error; and propagate all uncertainty in the vital rates into a probability distribution for the population growth rate and its sensitivities. Taken in isolation, any one of these features may be perceived as an incremental improvement over more traditional frequentist or maximum likelihood methods of IPM parameterization. We suggest, however, that their cumulative effect yields a quantitatively rigorous and satisfyingly probabilistic way to study population dynamics.

Furthermore, while many of these advantages would similarly apply to matrix models, the IPM framework facilitates more direct biological interpretation since life history functions are collected into vital rate sub-models that require far fewer parameters to be estimated from data. For example, we modeled spatial and temporal variance in survival via the intercept of a size-dependent func-

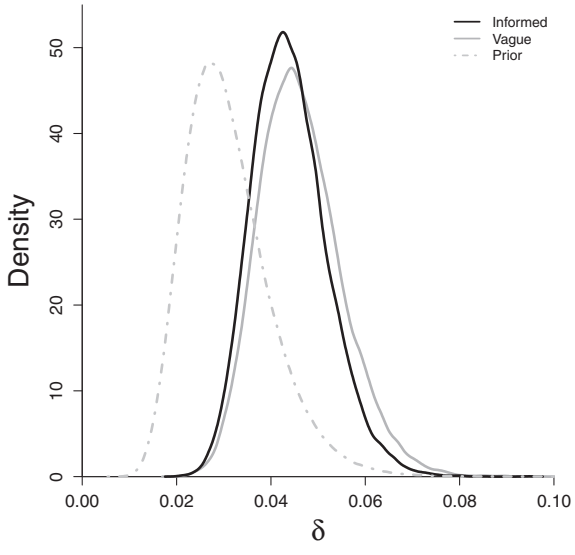

FIG. 5. Plot of the posterior densities of the plant-to-seedbank transition (δ) estimated using the vague prior (dark grey solid line) and the informed prior (black solid line). The prior distribution based on survey estimates is also plotted (dark grey dash-dot line).

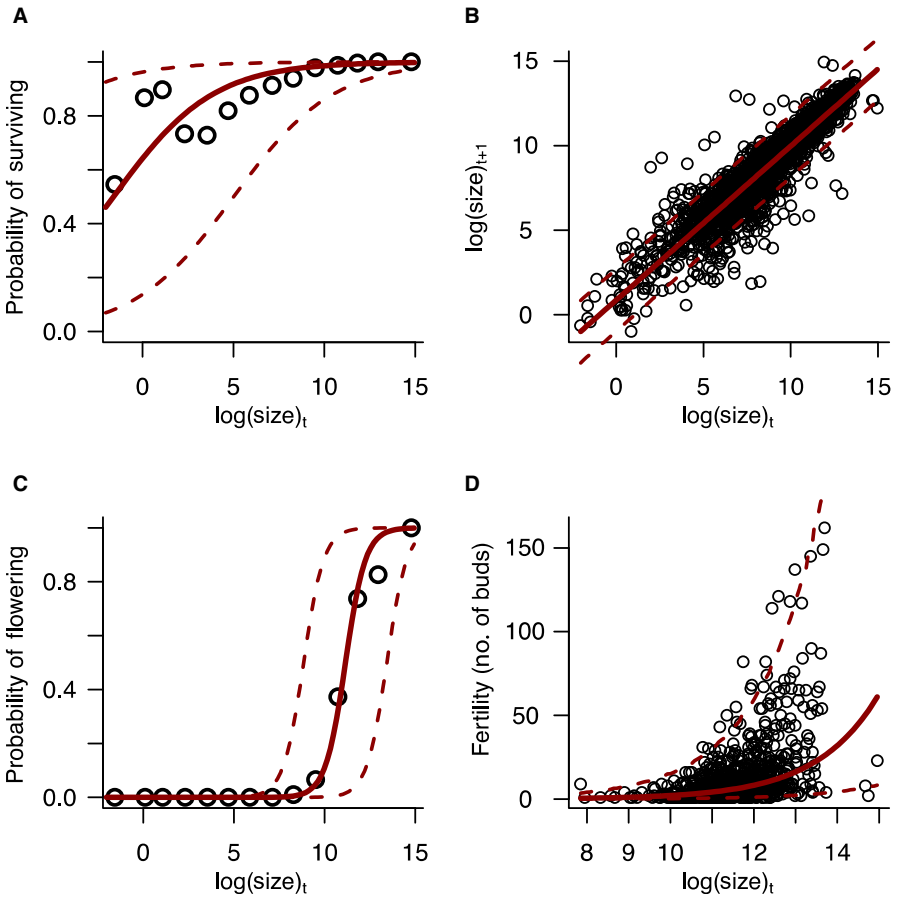

FIG. 6. Fit of the model to the data. The solid lines are the best fit lines and the dashed lines represent the 95% Prediction Intervals (PIs) for (A) survival, (B) growth, (C) probability of flowering, and (D) fertility. The PIs show the uncertainty associated with forecasting future estimates of the vital rate parameters. These estimates are often much wider than the associated Credible Intervals (CIs), which show the uncertainty associated with estimates of the mean (Appendix S1: Figure S2). In (A) and (C), points show binned means.

tion rather than considering the survival rates of different size classes as independent parameters, as in a matrix model. Thus, the parameter savings of an IPM combine powerfully with HB methods to quantify spatio-temporal heterogeneity, covariance, and uncertainty in vital rates per se.

A hierarchical Bayesian approach provides a natural solution to the problem of rigorously modeling the uncertainty in population level inferences, as the tree cholla data demonstrate. Demographic models are often constructed from a patchwork of different data sources. For tree cholla, building the IPM required that we combine data on the survival, growth, and reproduction of individuals marked for long-term census along with shorter-term observations of the seed content of fruits and germination, size, and survival of seedlings in seed addition experiments. We additionally used a prior probability informed by preliminary data and a latent-state modeling approach to infer a value for one component of the life cycle for which we had limited direct information, the maternal plant-to-seed bank transition. Each of these data sources included estimation uncertainty and one of them (the long-term census data) additionally included multiple sources of process error (spatial and temporal variability) with potential for correlated responses across vital rates. In our experience, the complexity of the tree cholla data is typical for demographic studies of natural populations. Ultimately, our goal as population ecologists is to draw inferences about the dynamics of our study populations from observations made at the level of individuals, with a population model (in this case, an IPM) as the vehicle of inference. Appropriately modeling the uncertainty in population-level inferences that stems from the uncertainty in each of the model's moving parts can be challenging with more common frequentist or maximum likelihood approaches and is often not even attempted given how cumbersome the process can be (Clark 2003). Because the Bayesian framework is explicitly grounded in probability, confidence in IPM predictions falls out of the analysis quite naturally.

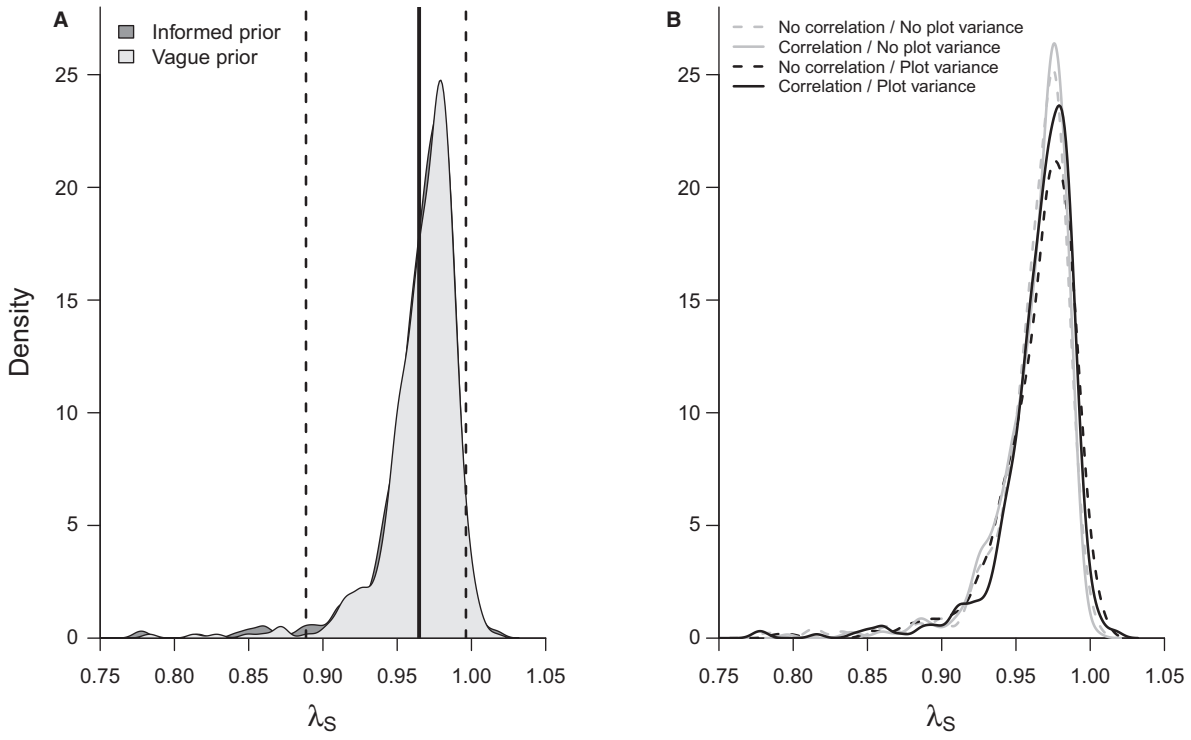

FIG. 7. (A) Posterior distribution of the tree cholla stochastic population growth rate (λ_S) based on an informed (dark gray) and vague (light gray) prior probability for the maternal plant-to-seed bank transition probability (Table 1). Solid and dashed vertical lines represent the mean and 95% CI, respectively, of λ_S, which were nearly identical between the informed and vague priors. (B) Posterior distribution for λ_S corresponding to each of four candidate models for demographic vital rates that include or exclude plot variability and temporal correlations (Table 2).

Differences in the methodologies between Bayesian and frequentist approaches also arise when interpreting the output. From a frequentist perspective, any quantity derived from the data, including population growth rate, represents an estimate of the "true" value of that parameter, which is fixed. The associated confidence intervals, often calculated via bootstrapping, only represent the uncertainty associated with measurement error, although non-Bayesian approaches have been developed to estimate both measurement and process errors (De Valpine and Hastings 2002). From a hierarchical Bayesian perspective, the estimate of population growth rate represents a random variable, which has an associated distribution. That is, there is no single "true" value and the population growth rate could take any value within the distribution. For example, some of the variability in λ_S (Fig. 7) reflects the fact that some plots are more favorable than others for population growth; this is biologically meaningful spatial heterogeneity that a Bayesian approach allows us to quantify. Interestingly, quantifying this source of variability suggested that spatial heterogeneity was generally less than temporal heterogeneity (Fig. 9) and contributed little to the total uncertainty in λ_S (Fig. 7B). Instead, most of the uncertainty was due to estimation error, or the variance in parameter estimates that arises from finite sampling. Temporal variability, per se, cannot affect the variance of λ_S because, for any amount of temporal variability, the stochastic growth rate converges on a single value (Eq. 12) in the absence of other sources of uncertainty (Tuljapurkar 1982). The dominance of estimation error in the posterior of λ_S suggests that our confidence in the population growth rate will become more finely resolved as the study continues and more data accumulate.

Estimation of process error is particularly important in the study of stochastic population dynamics, as the tree cholla data illustrate. All natural populations experience interannual variation in climate and stochastic events that vary from year to year such as fire, floods, outbreaks of natural enemies, etc. Understanding and predicting population trajectories in stochastic environments requires explicit consideration of the year-to-year variance (process error) in demographic vital rates (Caswell 2001, Rees and Ellner 2009). The HB perspective of vital rate parameters as random variables is therefore the necessary perspective of the stochastic demographer. Stochastic IPMs can be and have been built using maximum likelihood-based GLMMs for modeling temporal variation in vital rates (Williams and Crone 2006, Rees and Ellner 2009, Williams et al. 2015). This has the advantage of familiar, easy-to-use software for mixed modeling (e.g., lme4 in R, PROC GLIMMIX in SAS)

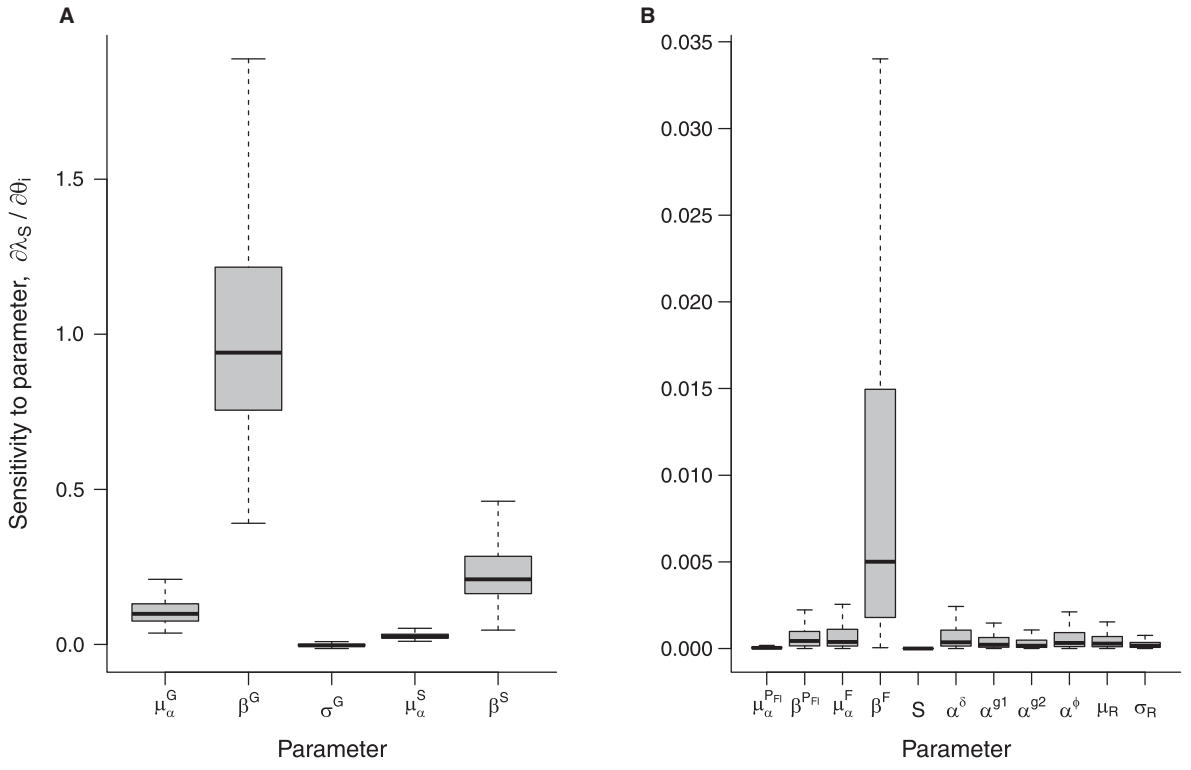

FIG. 8. Posterior distributions for the sensitivities of the stochastic growth rate to (A) parameter means ($\partial \lambda_S / \partial \theta_i$) for growth (superscript G) and survival (superscript S) parameters and (B) regeneration parameters, including probability of flowering (superscript P_{FI}) and fertility (superscript F); note different scales. Boxes show medians (thick black lines), inner quartiles (box borders), and 5 and 95 percentiles (whiskers) of sensitivity values derived from the joint posterior distribution of parameter values. Parameter symbols are the same as in Table 1.

as opposed to the customization that a Bayesian analysis requires. Thus, in some cases, the adequacy and relative ease of non-Bayesian approaches might make them a better option. However, maximum likelihood-based methods are less amenable to translating vital rate uncertainty into uncertainty in derived quantities (Figs. 6–8), which may be particularly important in applied contexts. Further, maximum likelihood methods may fail entirely for complex data structures. For example, modeling spatial process error and vital rate correlations in addition to temporal process error would have been much more challenging and perhaps impossible in a maximum likelihood context.

The posterior distribution for the stochastic growth rate (Fig. 7) allows us to make an explicitly probabilistic statement regarding tree cholla population dynamics: if the observed vital rates persist, the study population is projected to decline with nearly 100% probability. The study period (2004–2014) has included chronic drought and a severely cold winter in 2011, including all-time record low temperatures over a 4-day deep-freeze. Close inspection of the survival data indicated that the deep freeze likely caused 72% of all mortality events recorded during the entire study and that surviving plants had stunted growth. Thus, our relatively long-term study happened to include weather that was unusually harsh when considered in the context of the longer meteorological record. The occurrence of unusually bad years likely amplified the interannual variability in high-sensitivity vital rates, especially growth and survival (Fig. 8), which will generally decrease the stochastic population growth rate (Boyce et al. 2008). We hypothesize that, as the study continues and additional favorable years accumulate, the population growth rate will approach replacement levels.

While the hierarchical Bayesian framework works well with naturally hierarchical demographic data and can readily capture the uncertainty associated with spatiotemporal process error, this variability does not always translate to variability in population dynamics. In our study, the candidate model that accounted for spatiotemporal variability and vital rate correlations provided the best fit to the demographic data with a non-spatial model providing similar support (Table 2). Since these two models fit the data well, it is not surprising that their posterior distributions of λ_S are similar. However, the posterior distribution for λ_S was surprisingly unresponsive to temporal vital rate correlations (Fig. 7B). We hypothesize that this occurred because the vital rates that were most variable across time (as well as space) were also the vital rates to which population growth was least sensi-

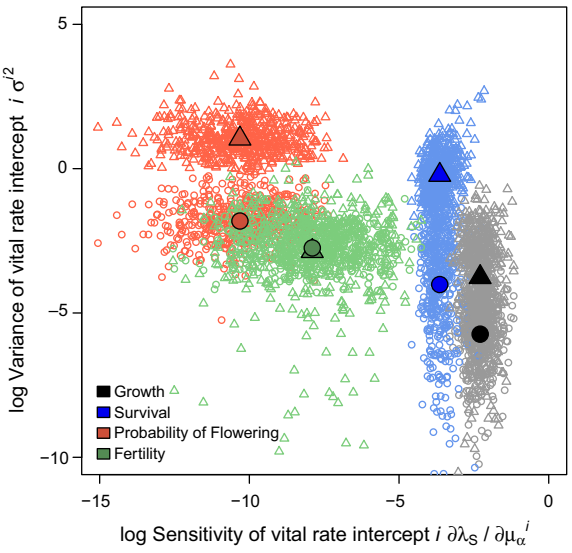

FIG. 9. The relationship between population growth rate sensitivity ($\partial \lambda_s / \partial \theta_i$) and spatio-temporal variability for each of the four vital rates estimated from long-term data (growth, survival, flowering, and fertility). Large filled symbols show posterior means for the spatial (circles) and temporal (triangles) variances (y-axis) of the vital rate intercepts in relation to their posterior mean sensitivities (x-axis). Point clouds show 500 draws from the posterior probability distributions. Note log-log scale.

tive (Fig. 9), a result predicted by theory and observed in other demographic studies (Pfister 1998, Pfister and Wang 2005). Thus, it is worth noting that much of the variability in individual demography so elegantly captured by a hierarchical Bayesian approach was relatively inconsequential at the population level. Whether this holds true for other species will depend on how they respond to spatio-temporal variation in survival, growth, and fecundity. Understanding the consequences of process variability can have valuable management implications.

As with all methods, there are potential limitations associated with the implementation of a hierarchical Bayesian approach. Some of the perils include assessing parameter convergence and the use of informed priors. With regard to the latter, unjustified informed priors represent bad choices and cannot be used alone to demean an approach. Also, use of an informed prior points to the importance of conducting a prior sensitivity analysis to determine just how much the prior influences the posterior estimates. In our study, we used preliminary data to define a prior probability for the maternal plant-to-seed bank transition, though we found that this informed prior was of little consequence (Fig. 7A). In other cases where preliminary data are not available, there may be additional data from other studies of the same species or closely related ones that can or should be used as prior information for demographic parameter estimation. Given that data are particularly precious for species of concern, combining data via priors also represents a distinct advantage of the Bayesian approach. With regards to other technical issues like assessing model selection, model fit, and parameter convergence, the needed Bayesian resources are expanding as instructional articles (Ellison 2004, Hobbs and Hilborn 2006, McCarthy 2007, Hooten and Hobbs 2015) and books (Clark 2007, McCarthy 2007, King et al. 2010, Kéry and Schaub 2012, Hobbs and Hooten 2015) continue to be published.

New Bayesian methods also continue to arise in the IPM literature. For example, work by Ghosh et al. (2012) uses point-pattern data to construct a Bayesian IPM, approaching estimation of the IPM kernel from an entirely different direction than presented here (and in the vast majority of IPM studies). Point-pattern data bypass individual-level vital rates and instead infer demographic transitions from changes in the population size structure from one time step to the next. Gelfand et al. (2013) use this method to show that point-pattern based IPMs can be used to scale up processes from the population to the region. In their paper, Ghosh et al. (2012) highlight some of the potential problems with IPMs relying on data from marked individuals and use this as a motivation for point-pattern approaches. The problem arises from computing population-level processes using the inappropriate scale of the individual (Ghosh et al. 2012). This is referred to as an "ecological fallacy" (Wakefield 2009) in which measurements taken at one scale are used to infer information at a larger scale. As Ellner (2012) points out in the commentary on Ghosh et al. (2012), this mean-field approach is standard practice for most IPMs including the cholla models presented here as well as most other demographic matrix models (but see Forbis and Doak 2004). While there is still much to be debated about the different methods, the way forward may be to combine the individual-level vital rate data and the population size structure data to infer something about individual processes as well as population processes (Ellner 2012). This hybrid of individual- and population-level data represents another area in which HB methods can excel given the strengths of the method in combining multiple data sets (Clark 2007, Hobbs and Hooten 2015).

Lastly, methods associated with Bayesian model selection are rapidly developing, which may increase the wariness of potential users but also represents the development of new and exciting tools. The most appropriate model selection criterion will depend on the data, the model, and the research questions (Hooten and Hobbs 2015). One of the most common criteria for Bayesian model selection is the DIC (Spiegelhalter et al. 2002), which works when comparing linear models but, as noted earlier, tends to favor more complicated models. The recently developed WAIC allows for a fully Bayesian comparison between models (Watanabe 2013) and is recommended for use when comparing hierarchical models. However, WAIC does not perform well with models that account for spatial and temporal variability (Hooten and Hobbs 2015). To compare the candidate models, we chose to use cross-validation. While this approach is

computationally expensive and, thus, not always feasible, cross-validation provides a good means of determining a model's predictive ability. Clearly, no single model selection approach may be ideal for all data sets and questions. We refer the reader to Hooten and Hobbs (2015), which provides an excellent overview of current guidelines to Bayesian model selection.

Rather than selecting the best model, population demographers may want to combine the strength of a set of models or focus on model averaging. Reversible-jump Markov chain Monte Carlo (RJMCMC) is a computational algorithm that averages across models (King et al. 2010, Barker and Link 2013). For RJMCMC, the MCMC chain includes a step that allows for switching between candidate models. For example, to conduct an RJMCMC for the cholla data, at each step the chain would choose between one of the four models considered in Table 2. The limited use of RJMCMC may have stemmed from problems of implementation for complicated models (Hooten and Hobbs 2015). Barker and Link (2013) recently proposed an easily implemented solution to this problem by using the MCMC samples from each model fit in a *post-hoc* analysis.

In conclusion, IPMs helped solve the problems associated with dividing continuous demographic states into discrete classes. A hierarchical Bayesian framework enhances the utility of the IPM approach by accommodating multiple data sets, incorporating complex variance structures, and robustly accounting for various aspects of uncertainty associated with demographic parameters. In turn, Bayesian parameter estimates can be used to calculate robust probability distributions for standard demographic metrics such as population growth rate and its sensitivities or elasticities. Overall, by building along a hierarchical framework, Bayesian approaches provide a statistically sound way to get more information out of precious demographic data.

Acknowledgements

We thank J. HilleRisLambers, S. Kroiss, B. Van Allen, F. Dillemuth, A. Flick, and the Beer Bayes group at Rice University for helpful discussion and comments on the manuscript. B. Ochocki provided valuable computational assistance and advice. We would also like to thank M. Hooten and an anonymous reviewer for their comments, which greatly improved the manuscript. We thank the many students who have contributed to the tree cholla demographic study and acknowledge the support of the Sevilleta National Wildlife Refuge and Sevilleta Long Term Ecological Research (NSF DEB-0620482 and DEB-1232294). Our statistical and demographic research was supported by NSF-DEB-1316334 (BDE) and NSF-DEB-1145588 and DEB-1543651 (TEXM).

Literature Cited

Barker, R. J., and W. A. Link. 2013. Bayesian multimodel inference by RJMCMC: a Gibbs sampling approach. American Statistician 67:150–156.

Bolker, B. M., M. E. Brooks, C. J. Clark, S. W. Geange, J. R. Poulsen, M. H. H. Stevens, and J. S. S. White. 2009. Generalized linear mixed models: a practical guide for ecology and evolution. Trends in Ecology & Evolution 24:127–135.

Boyce, M. S., C. V. Haridas, C. T. Lee, and NCEAS Stochastic Demography Working Group. 2006. Demography in an increasingly variable world. Trends in Ecology & Evolution 21:141–148.

Brooks, S. P., and A. Gelman. 1998. General methods for monitoring convergence of iterative simulations. Journal of Computational and Graphical Statistics 7:434–455.

Caswell, H. 2001. Matrix population models: construction, analysis, and interpretation. Sinauer Associates, Sunderland, Massachusetts, USA.

Childs, D. Z., T. N. Coulson, J. M. Pemberton, T. H. Clutton-Brock, and M. Rees. 2011. Predicting trait values and measuring selection in complex life histories: reproductive allocation decisions in Soay sheep. Ecology Letters 14:985–992.

Clark, J. S. 2003. Uncertainty and variability in demography and population growth: a hierarchical approach. Ecology 84:1370–1381.

Clark, J. S. 2007. Models for ecological data: an introduction. Princeton University Press, Princeton, New Jersey, USA.

Clark, J. S., and A. E. Gelfand. 2006. A future for models and data in environmental science. Trends in Ecology & Evolution 21:375–380.

Clark, J. S., G. A. Ferraz, N. Oguge, H. Hays, and J. DiCostanzo. 2005. Hierarchical Bayes for structured, variable populations: from recapture data to life-history prediction. Ecology 86:2232–2244.

Coulson, T. 2012. Integral projections models, their construction and use in posing hypotheses in ecology. Oikos 121:1337–1350.

Coulson, T., D. R. MacNulty, D. R. Stahler, B. vonHoldt, R. K. Wayne, and D. W. Smith. 2011. Modeling effects of environmental change on wolf population dynamics, trait evolution, and life history. Science 334:1275–1278.

Cressie, N. 1993. Statistics for spatial data. John Wiley & Sons, Hoboken, New Jersey, USA.

Cressie, N., C. A. Calder, J. S. Clark, J. M. Ver Hoef, and C. K. Wikle. 2009. Accounting for uncertainty in ecological analysis: the strengths and limitations of hierarchical statistical modeling. Ecological Applications 19:553–570.

Crouse, D. T., L. B. Crowder, and H. Caswell. 1987. A stage-based population-model for Loggerhead Sea Turtles and implications for conservation. Ecology 68:1412–1423.

Dantin, M. R. T., and M. Fortin. 2014. Spatial analysis: a guide for ecologists. Cambridge University Press, Cambridge, UK.

Davis, A. J., M. B. Hooten, M. L. Phillips, and P. F. Doherty. 2014. An integrated modeling approach to estimating Gunnison sage-grouse population dynamics: combining index and demographic data. Ecology and Evolution 4:4247–4257.

De Valpine, P., and A. Hastings. 2002. Fitting population models incorporating process noise and observation error. Ecological Monographs 72:57–76.

Dennis, B. 1996. Discussion: Should ecologists become Bayesians? Ecological Applications 6:1095–1103.

Dennis, B., P. L. Munholland, and J. M. Scott. 1991. Estimation of growth and extinction parameters for endangered species. Ecological Monographs 61:115–143.

Diez, J. M., I. Giladi, R. Warren, and H. R. Pulliam. 2014. Probabilistic and spatially variable niches inferred from demography. Journal of Ecology 102:544–554.

Doak, D. F. 1995. Source-sink models and the problem of habitat degradation: general models and applications to the Yellowstone grizzly. Conservation Biology 9:1370–1379.

Doak, D., P. Kareiva, and B. Kleptetka. 1994. Modeling population viability for the desert tortoise in the Western Mojave Desert. Ecological Applications 4:446–460.

Doak, D. F., W. F. Morris, C. Pfister, B. E. Kendall, and E. M. Bruna. 2005. Correctly estimating how environmental stochasticity influences fitness and population growth. American Naturalist 166:E14–E21.

Easterling, M. R., S. P. Ellner, and P. M. Dixon. 2000. Size-specific sensitivity: applying a new structured population model. Ecology 81:694–708.

Elderd, B. D., G. Dwyer, and V. Dukic. 2013. Population-level differences in disease transmission: a Bayesian analysis of multiple smallpox epidemics. Epidemics 5:146–156.

Ellison, A. M. 1996. An introduction to Bayesian inference for ecological research and environmental decision-making. Ecological Applications 6:1036–1046.

Ellison, A. M. 2004. Bayesian inference in ecology. Ecology Letters 7:509–520.

Ellner, S. P. 2012. Comments on: inference for size demography from point process data using integral projection models. Journal of Agricultural Biological and Environmental Statistics 17:682–689.

Ellner, S. P., and M. Rees. 2006. Integral projection models for species with complex demography. American Naturalist 167:410–428.

Evans, M. E. K., and K. E. Holsinger. 2012. Estimating covariation between vital rates: a simulation study of connected vs. separate generalized linear mixed models (GLMMs). Theoretical Population Biology 82:299–306.

Evans, M. E. K., K. E. Holsinger, and E. S. Menges. 2010. Fire, vital rates, and population viability: a hierarchical Bayesian analysis of the endangered Florida scrub mint. Ecological Monographs 80:627–649.

Forbis, T. A., and D. F. Doak. 2004. Seedling establishment and life history trade-offs in alpine plants. American Journal of Botany 91:1147–1153.

Franklin, A. B., D. R. Anderson, R. J. Gutierrez, and K. P. Burnham. 2000. Climate, habitat quality, and fitness in Northern Spotted Owl populations in northwestern California. Ecological Monographs 70:539–590.

Gelfand, A. E., S. Ghosh, and J. S. Clark. 2013. Scaling integral projection models for analyzing size demography. Statistical Science 28:641–658.

Gelman, A. 2006. Prior distributions for variance parameters in hierarchical models. Bayesian Analysis 1:515–533.

Gelman, A., and J. Hill. 2007. Data analysis using regression and multilevel/hierarchical models. Cambridge University Press, Cambridge, UK.

Gelman, A., X. L. Meng, and H. Stern. 1996. Posterior predictive assessment of model fitness via realized discrepancies. Statistica Sinica 6:733–760.

Gelman, A., J. B. Carlin, H. S. Stern, and D. B. Rubin. 2003. Bayesian data analysis. Chapman and Hall, Boca Raton, Florida, USA.

Gelman, A., J. Hwang, and A. Vehtari. 2014. Understanding predictive information criteria for Bayesian models. Statistics and Computing 24:997–1016.

Ghosh, S., A. E. Gelfand, and J. S. Clark. 2012. Inference for size demography from point pattern data using integral projection models. Journal of Agricultural Biological and Environmental Statistics 17:641–677.

Grimm, V. 2005. Individual-based modeling and ecology. Princeton University Press, Princeton, New Jersey, USA.

Hanks, E. M., M. B. Hooten, and F. A. Baker. 2011. Reconciling multiple data sources to improve accuracy of large-scale prediction of forest disease incidence. Ecological Applications 21:1173–1188.

Heidelberger, P., and P. D. Welch. 1983. Simulation run length control in the presence of an initial transient. Operations Research 31:1109–1144.

Hille Ris Lambers, J., J. S. Clark, and M. Lavine. 2005. Implications of seed banking for recruitment of southern Appalachian woody species. Ecology 86:85–95.

Hobbs, N. T., and R. Hilborn. 2006. Alternatives to statistical hypothesis testing in ecology: a guide to self teaching. Ecological Applications 16:5–19.

Hobbs, N. T., and M. B. Hooten. 2015. Bayesian models: a statistical primer for ecologists. Princeton University Press, Princeton, New Jersey, USA.

Hobbs, N. T., C. Geremia, J. Treanor, R. L. Wallen, P. J. White, M. B. Hooten, and J. C. Rhyan. 2015. State-space modeling to support management of brucellosis in the Yellowstone bison population. Ecological Monographs 85:525–556.

Hooten, M. B., and N. T. Hobbs. 2015. A guide to Bayesian model selection for ecologists. Ecological Monographs 85:3–28.

Huang, A., and M. P. Wand. 2013. Simple marginally noninformative prior distributions for covariance matrices. Bayesian Analysis 8:439–451.

Kéry, M. 2010. Introduction to WinBUGS for ecologists. Academic Press, Boston, Massachusetts, USA.

Kéry, M., and M. Schaub. 2012. Bayesian population analysis using WinBUGS. Academic Press, Boston, Massachusetts, USA.

King, R., B. J. T. Morgan, O. Gimenez, and S. P. Brooks. 2010. Bayesian analysis for population ecology. Chapman and Hall, Boca Raton, Florida, USA.

Kuss, P., M. Rees, H. H. Aegisdottir, S. P. Ellner, and J. Stocklin. 2008. Evolutionary demography of long-lived monocarpic perennials: a time-lagged integral projection model. Journal of Ecology 96:821–832.

Ladeau, S. L., and J. S. Clark. 2006. Elevated CO2 and tree fecundity: the role of tree size, interannual variability, and population heterogeneity. Global Change Biology 12:822–833.

Lefkovitch, L. P. 1965. Study of population growth in organisms grouped by stages. Biometrics 21:1–18.

Leslie, P. H. 1945. On the use of matrices in certain population mathematics. Biometrika 33:183–212.

Link, W. A., and R. J. Barker. 2010. Bayesian inference with ecological applications. Academic Press, Boston, Massachusetts, USA.

Link, W. A., and M. J. Eaton. 2012. On thinning of chains in MCMC. Methods in Ecology and Evolution 3:112–115.

McCarthy, M. A. 2007. Bayesian methods for ecology. Cambridge University Press, Cambridge, UK.

McEvoy, P. B., and E. M. Coombs. 1999. Biological control of plant invaders: regional patterns, field experiments, and structured population models. Ecological Applications 9:387–401.

Merow, C., J. P. Dahlgren, C. J. E. Metcalf, D. Z. Childs, M. E. K. Evans, E. Jongejans, S. Record, M. Rees, R. Salguero-Gomez, and S. M. McMahon. 2014a. Advancing population ecology with integral projection models: a practical guide. Methods in Ecology and Evolution 5:99–110.

Merow, C., A. M. Latimer, A. M. Wilson, S. M. McMahon, A. G. Rebelo, and J. A. Silander. 2014b. On using integral projection models to generate demographically driven predictions of species' distributions: development and validation using sparse data. Ecography 37:1167–1183.

Metcalf, C. J. E., S. M. McMahon, R. Salguero-Gomez, and E. Jongejans. 2013. IPMpack: an R package for integral projection models. Methods in Ecology and Evolution 4:195–200.

Miller, T. E. X., S. M. Louda, K. A. Rose, and J. O. Eckberg. 2009. Impacts of insect herbivory on cactus population dynamics: experimental demography across an environmental gradient. Ecological Monographs 79:155–172.

Miller, T. E. X., J. L. Williams, E. Jongejans, R. Brys, and H. Jacquemyn. 2012. Evolutionary demography of iteroparous plants: incorporating non-lethal costs of reproduction into

integral projection models. Proceedings of the Royal Society B 279:2831–2840.
Moloney, K. A. 1986. A generalized algorithm for determining category size. Oecologia 69:176–180.
Morris, W. F., and D. F. Doak. 2002. Quantitative conservation biology: theory and practice of population viability analysis. Sinauer Associates, Sunderland, Massachusetts, USA.
Ohm, J. R., and T. E. X. Miller. 2014. Balancing anti-herbivore benefits and anti-pollinator costs of defensive mutualists. Ecology 95:2924–2935.
Parker, I. M. 2000. Invasion dynamics of *Cytisus scoparius*: a matrix model approach. Ecological Applications 10:726–743.
Pfister, C. A. 1998. Patterns of variance in stage-structured populations: evolutionary predictions and ecological implications. Proceedings of the National Academy of Sciences 95:213–218.
Pfister, C. A., and M. Wang. 2005. Beyond size: matrix projection models for populations where size is an incomplete descriptor. Ecology 86:2673–2683.
Plummer, M., N. Best, K. Cowles, and K. Vines. 2006. CODA: convergence diagnosis and output analysis for MCMC. R News 6:7–11.
R Core Team. 2013. R: a language and environment for statistical computing. R Foundation for Statistical Computing, Vienna, Austria.
Rees, M., and S. P. Ellner. 2009. Integral projection models for populations in temporally varying environments. Ecological Monographs 79:575–594.
Rees, M., D. Z. Childs, and S. P. Ellner. 2014. Building integral projection models: a user's guide. Journal of Animal Ecology 83:528–545.
Ruete, A., K. Wiklund, and T. Snall. 2012. Hierarchical Bayesian estimation of the population viability of an epixylic moss. Journal of Ecology 100:499–507.
Spiegelhalter, D. J., N. G. Best, B. R. Carlin, and A. van der Linde. 2002. Bayesian measures of model complexity and fit. Journal of the Royal Statistical Society Series B 64:583–616.
Su, Y., and M. Yajima. 2014. R2jags: a package for running jags from R. https://cran.r-project.org/web/packages/R2jags/index.html
Tuljapurkar, S. D. 1982. Population-dynamics in variable environments. III. Evolutionary dynamics of r-selection. Theoretical Population Biology 21:141–165.
Vandermeer, J. 1978. Choosing category size in a stage projection matrix. Oecologia 32:79–84.
Wakefield, J. 2009. Multi-level modelling, the ecologic fallacy, and hybrid study designs. International Journal of Epidemiology 38:330–336.
Wallace, K., A. Leslie, and T. Coulson. 2013. Re-evaluating the effect of harvesting regimes on Nile crocodiles using an integral projection model. Journal of Animal Ecology 82:155–165.
Walters, C. J. 1986. Adaptive management of renewable resources. MacMillan Publishing, New York, New York, USA.
Watanabe, S. 2013. A widely applicable Bayesian information criterion. Journal of Machine Learning Research 14:867–897.
Wikle, C. K. 2002. A kernel-based spectral model for non-Gaussian spatio-temporal processes. Statistical Modelling 2:299–314.
Wikle, C. K., and M. B. Hooten. 2010. A general science-based framework for dynamical spatio-temporal models. Test 19:417–451.
Williams, J. L., and E. E. Crone. 2006. The impact of invasive grasses on the population growth of *Anemone patens*, a long-lived native forb. Ecology 87:3200–3208.
Williams, J. L., T. E. X. Miller, and S. P. Ellner. 2012. Avoiding unintentional eviction from integral projection models. Ecology 93:2008–2014.
Williams, J. L., H. Jacquemyn, B. Ochocki, R. Brys, and T. E. X. Miller. 2015. Life history evolution under climate change and its influence on the population dynamics of a long-lived plant. Journal of Ecology 103:798–808.

Supporting Information

Additional supporting information may be found in the online version of this article at http://onlinelibrary.wiley.com/doi/10.1890/15-1526.1/suppinfo

Data Availability

Data associated with this paper have been deposited in Dryad: http://dx.doi.org/10.5061/dryad.db428